Transition-State Solvent Effects on Atom Transfer Rates in Solution

Branka M. Ladanyi*[†] and James T. Hynes*[‡]

Contribution from the Department of Chemistry, Colorado State University, Fort Collins, Colorado 80523, and the Department of Chemistry, University of Colorado, Boulder, Colorado 80309. *Received April 2, 1985*

Abstract: The static "caging" effect of an inert solvent on the rates of atom-transfer reactions is studied theoretically. In addition to their intrinsic interest, these effects are important in isolating the solvent "dynamic" influence on solution rates. Calculated variational transition-state theory rates for the model H exchange reaction between methyl radical and methane are compared in the gas phase and in model compressed Ar and Xe solvents over a wide pressure range. The calculated solvent enhancement of the rate varies with solvent, pressure, and reaction system and can reach up to several orders of magnitude. Calculated activation volumes vary strongly with pressure and bear little relation to values calculated solely in terms of geometric changes on passage to the transition state. The solvent rate enhancement is found to be much less for simple geometric isomerizations. But it is pointed out that the observed variation of the volume of activation with pressure can play an important role in the interpretation of experimental rates in terms of dynamic solvent effects.

The influence of a solvent on the rates of chemical reactions in solution is most often interpreted theoretically in terms of transition-state theory (TST).[1,2] The most frequent and well-known application of TST ideas is to solution reactions involving charges and dipoles in polar solvents.[2-4] A less frequent application but nonetheless one of fundamental chemical importance is to bimolecular atom-transfer rates in solution

$$A + BC \rightarrow AB + C \qquad (1)$$

In this paper, we examine the equilibrium static influence of an inert nonpolar solvent on the rates of model H-atom-transfer reactions.

The thermodynamic formulation[1,2] of TST provides the most commonly applied and convenient basis for analysis of solution rates. It focuses attention on the solvent effects on the activation free energy $\Delta G^{\ddagger} = G^{\ddagger} - G^{R}$, i.e., the difference of transition-state and reactant free energies. If for example solvation stabilizes the transition state more than it stabilizes the reactants, the reaction is accelerated compared to the gas phase. This thermodynamic route to solvent reaction effects has been followed along many branches in the past for atom-transfer reactions,[3] and an impressively wide range of concepts—such as free volume,[3a,c,g] solubilities,[3f,g] transition-state "boiling points",[3e] and Bunsen absorption coefficients[3d]—have been invoked in its implementation. Although these approaches have often been useful in qualitatively explaining trends observed in experimental data, they have been less successful in obtaining quantitative predictions of solvent effects on reaction rates. One reason for this lack of success is that the ingredients required—such as transition-state boiling points and solubilities—are not measurable and are difficult to estimate accurately. A further reason is that macroscopic concepts are often invoked in these approaches when dealing with molecular level quantities. Free volume theory, used to estimate the effects of solvent packing, is an example of this type of approximation. Moreover, these approaches have usually ignored the effects of short-range steric interactions, which strongly influence structural and thermodynamic properties of dense fluids. Thus theoretical estimates of the solvent acceleration of solution bimolecular reaction rates range from a factor of about unity (i.e., no effect) to a factor of 100. A more fundamental molecular approach to this problem is required in order to overcome these difficulties.

The procedure we follow in this paper is both simple and direct. We employ the equilibrium theory of solvent structure and thermodynamics,[5] combined with variational TST,[6] to calculate rates. We will find that the rate acceleration depends on both the reaction system and the solvent and can be quite dramatic—reaching up to several orders of magnitude.

We will focus our attention on H-atom-transfer reactions AH + B → A + HB in this initial effort for three reasons. First, the small size of H compared to typical A and B moieties reduces the problem approximately to the consideration of the interaction solely of A and B with the solvent (see below). Second, the compact nature of the typical transition state of an AHB system leads to rather large solvent effects. Finally, detailed gas-phase calculations for these reactions are available[7] for comparison with our solution results.

We stress at the outset that we are concerned here solely with *equilibrium* solvent effects on rates, within a TST framework. The possibility of the breakdown of TST itself due to solvent dynamics is a separate and critical question attracting considerable recent interest,[8] but it is not addressed here. Nonetheless it is worth stressing that static solvent effects need to be sorted out before any dynamic solvent influences on rates can be clearly revealed.[8b]

[†]Colorado State University. Alfred P. Sloan Fellow and Camille and Henry Dreyfus Teacher-Scholar.
[‡]University of Colorado.

(1) (a) Glasstone, S.; Laidler, K.; Eyring, H. "The Theory of Rate Processes"; McGraw-Hill: New York, 1941. (b) Evans, M. G.; Polanyi, M. *Trans. Faraday Soc.* **1935**, *31*, 875. (c) Wynne-Jones, W. F. K.; Eyring, H. *J. Chem. Phys.* **1935**, *3*, 492.

(2) (a) Entelis, S. G.; Tiger, R. P. "Reaction Kinetics in the Liquid Phase": Wiley: New York, 1976. (b) Reichardt, C. "Solvent Effects in Organic Chemistry"; Verlag-Chemie: New York, 1979.

(3) (a) Benson, S. W. "The Foundation of Chemical Kinetics"; McGraw-Hill: New York, 1960. (b) Moelwyn-Hughes, E. A. "The Chemical Statics and Kinetics of Solutions"; Academic: London, 1971. (c) Frost, A. A.; Pearson, R. F. "Kinetics and Mechanism", 2nd ed.; Wiley: New York, 1961. (d) Weston, R. E.; Schwarz, H. A. "Chemical Kinetics"; Prentice-Hall: Englewood Cliffs, NJ, 1972. (e) Benson, S. W.; Golden, D. M. In "Physical Chemistry. An Advanced Treatise" **1975**, *7*, 57. (f) Bell, R. P. *Annu. Rep. Prog. Chem.* **1939**, *36*, 82; *Trans. Faraday Soc.* **1939**, *35*, 324. (g) Martin, H. *Angew. Chem., Int. Ed. Engl.* **1966**, *5*, 78. (h) Mayo, F. R. *J. Am. Chem. Soc.* **1967**, *89*, 2654. (i) Stein, S. *Ibid.* **1981**, *103*, 5685.

(4) Several recent studies employ mean potential techniques similar to the present study in S_N2 reactions: (a) Chandrasekhar, J.; Smith, S. F.; Jorgensen, W. L. *J. Am. Chem. Soc.* **1984**, *106*, 3049; **1985**, *107*, 154. (b) Chiles, R. A.; Rossky, P. J. *Ibid.* **1984**, *106*, 6867. For a model association reaction study, see: (c) Cummings, P. T.; Stell, G. *Mol. Phys.* **1984**, *51*, 253.

(5) For reviews, see: (a) Chandler, D. In "The Liquid State of Matter: Fluids, Simple and Complex"; Montroll, E. W., Lebowitz, J. L., Eds.; North Holland: Amsterdam, 1982. (b) Ben-Naim, A. "Hydrophobic Interactions": Plenum: New York, 1980.

(6) For reviews, see: Truhlar, D. G.; Garrett, B. C. *Acc. Chem. Res.* **1980**, *13*, 440; *Annu. Rev. Phys. Chem.* **1984**, *35*, 159.

(7) (a) Garrett, B. C.; Truhlar, D. G. *J. Am. Chem. Soc.* **1979**, *101*, 4534. (b) Garrett, B. C.; Truhlar, D. G.; Wagner, A. F.; Dunning, T. H. *J. Chem. Phys.* **1983**, *78*, 4400. Bondi, D. K.; Connor, J. N. L.; Garrett, B. C.; Truhlar, D. G. *Ibid.* **1983**, *78*, 5981. Truhlar, D. G.; Garrett, B. C.; Hipes, P. G.; Kuppermann, A. *Ibid.* **1984**, *81*, 3542.

(8) (a) Truhlar, D. G.; Hase, W. L.; Hynes, J. T. *J. Phys. Chem.* **1983**, *87*, 2664. (b) Hynes, J. T. In "The Theory of Chemical Reactions"; Baer, M., Ed.; CRC Press: Boca Raton, FL, 1985; Vol. 4, p 171.

0002-7863/86/1508-0585$01.50/0

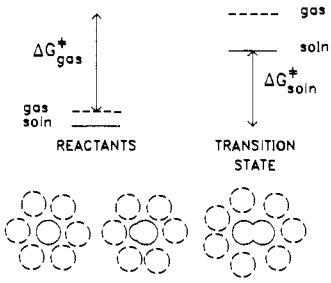

Figure 1. Free energy stabilization of the transition state in solution by the solvent compared to the gas phase. The bottom portion of the figure qualitatively indicates the solvent "pressure" effect on the compact transition state, in contrast to the negligible effect on the separated reactants. The reacting A, H, and B moieties are overlapped in the approximate way shown in the transition state (see the text).

The outline of this paper is as follows. We first describe our theoretical formulation. We then present and discuss our results for atom transfers. We next briefly address the analogous problem for isomerizations. A summary concludes the paper.

Theory

Gas- and Solution-Phase Rate Constants. The TST expression for the rate constant for a gas-phase collinear atom transfer is well-known[1,7]

$$k_{gas} = \sigma_{rx}\frac{k_B T}{h}\frac{Q^{\ddagger}}{(Q^R/V)}e^{-U^{\ddagger}/RT} \tag{2}$$

Here $U^{\ddagger}$ is the molar potential energy at the transition state, with the separated reactants assigned as the zero of energy. Q^R/V is the partition function (pf) of the separated reactants per unit volume, and $Q^{\ddagger}$ is the pf of the transition state excluding both translation and motion along the reaction coordinate. Zero-point vibrational energy factors are included in both Q^R and $Q^{\ddagger}$. Finally, σ_{rx} is the number of equivalent reaction paths from reactants to products (e.g., two for an atom–homonuclear diatom reaction and one for an atom–heteronuclear diatom reaction).[7] Equation 2 refers to the rate constant in a concentration rate law.

The thermodynamic version of the gas-phase result eq 2 is also well-known[1,6,7]

$$k_{gas} = (k_B T/h)K^{\circ}e^{-\Delta G^{\ddagger}_{gas}/RT} \tag{3}$$

Here $\Delta G^{\ddagger}_{gas}$ is the Gibbs free energy of activation and K° is the reciprocal of the constant standard-state concentration.

If we now turn to the solution-phase reaction, the analogue of eq 3 is simply

$$k_{soln} = (k_B T/h)K^{\circ}e^{-\Delta G^{\ddagger}_{soln}/RT} \tag{4}$$

at the same temperature and with the same standard-state concentration definition. Figure 1 illustrates schematically the solvent effect that we anticipate for simple atom transfers in inert solvents. Imagine for simplicity that the solvent molecules interact with the reaction system as hard spheres. The "pressure" of the high-density solvent will tend to make the compact transition state more favorable, i.e., more probable, compared to the gas phase in an effect akin to Le Châtelier's principle predictions.[3a] (The precise meaning of this simplified "pressure" terminology will be discussed below). Thus the free energy of the transition state will be lowered as the solvent density increases. But this effect will be typically much smaller for the reactants. Indeed, if A and HB were simply rigid spheres as far as their interaction with the solvent were concerned, there would be no effect at all on the reactants, since a reduction in pressure by forming a more compact structure would be impossible. Further, an inert solvent should only produce a modest shift in the high-frequency HB vibration.[9]

Thus the simple hard-sphere picture suggests a lowering of the free energy of activation in solution, $\Delta G^{\ddagger}_{soln} < \Delta G^{\ddagger}_{gas}$, and a resulting acceleration of the reaction rate. This is the static "caging" effect that we will calculate.

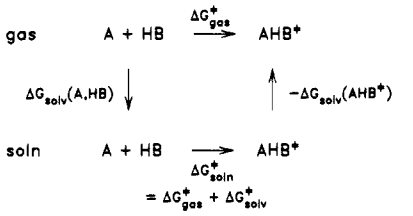

Figure 2. Free energy diagram illustrating the meaning of the free energy terms $\Delta G^{\ddagger}_{gas}$, $\Delta G^{\ddagger}_{soln}$, and $\Delta G^{\ddagger}_{solv}$. In the present approach, $\Delta G^{\ddagger}_{solv}$ is determined from the rate constants for the gas- and solution-phase reactions. A more traditional approach[1-3] typically focuses on the solvation free energies ΔG_{solv}(A,HB) and ΔG_{solv}(AHB‡).

Henceforward we specialize to the AHB case of H-atom transfer between larger, heavier groups A and B. The size of H is small compared to that of typical A and B groups such as CH_3, and to a first approximation we can ignore the interaction of H with the inert solvent. The inner H atom is "shielded" from the solvent in the transition-state region by the larger flanking A and B groups. To clarify ideas, we can for the moment proceed with the following simplified description. From the point of view of the solvent, the reaction involves bringing the separated A and HB species together to the transition-state configuration, with only A and B in interaction with the solvent. The free energy change for this process is approximately

$$\Delta G^{\ddagger}_{soln} = \Delta G^{\ddagger}_{gas} + \Delta w^{\ddagger}_{AB}(r^{\ddagger}_{AB}) \equiv \Delta G^{\ddagger}_{gas} + \Delta G^{\ddagger}_{solv} \tag{5}$$

Here $\Delta w^{\ddagger}_{AB}(r^{\ddagger}_{AB}) = \Delta G_{solv}$ is the *solvent contribution to the potential of mean force*, i.e., the solvent contribution to the molar free energy change on bringing together A and B up to the transition state separation $r^{\ddagger}_{AB}$ from infinite separation $r_{AB} = \infty$ in the solvent. As is well-known,[5,10] this mean potential is related to the pair distribution function $g_{AB}(r_{AB})$ at any separation by

$$g_{AB}(r_{AB}) = g^{\circ}_{AB}(r_{AB})e^{-\Delta w_{AB}(r_{AB})/RT} \tag{6}$$

where g°_{AB} is the pair distribution of the absence of the solvent, i.e., the exponential of minus the intrinsic molar A–B interaction potential energy divided by RT. It then follows from eq 3–5 that the ratio of solution- to gas-phase rate constants is simply[8b]

$$k_{soln}/k_{gas} = e^{-\Delta G^{\ddagger}_{solv}/RT} \tag{7}$$

This can be calculated if we know $\Delta w^{\ddagger}_{AB}(r^{\ddagger}_{AB})$, and this will in essence be our goal. A molecular theory for the problem of chemical equilibria in solution has been developed by Chandler and Pratt.[11] In this paper we extend this theory to static solvation effects on reaction rates. Figure 2 contrasts the approach used here, which deals directly with $\Delta G^{\ddagger}_{solv}$, with solution thermodynamic approaches[2,3] that focus separately on the solvation of the reactants and the transition state. [Occasionally, solvent effects on bimolecular neutral reactions are discussed in terms of, and attributed to, the increase in collision frequency between reactants in solution.[3b,c,f] But, as discussed by Northrup and Hynes[12] and Hynes,[8b] this interpretation is fundamentally incorrect for activated reactions, due to the neglect of solvent effects on the activation free energy from the reactant collision radius.]

Theoretical Model. The discussion above has been considerably oversimplified for clarity. In order to describe the actual calculation of the rate constant ratio k_{soln}/k_{gas}, we need to specify the calculation of k_{gas} in considerably more detail. To proceed, we need first to consider some of the key ideas of variational transition-state theory (VTST).[6,7]

(9) For example, even lower frequency ($\simeq$2670 cm^{-1}) and more polar OD vibrations are negligibly shifted in inert solvents: Kagiya, T.; Sumida, Y.; Inove, T. *Bull. Chem. Soc. Jpn.* **1968**, *41*, 767.

(10) (a) Hill, T. L. "Statistical Mechanics"; McGraw-Hill: New York, 1956. (b) McQuarrie, D. A. "Statistical Mechanics"; Harper & Row: New York, 1976.

(11) (a) Chandler, D.; Pratt, L. R. *J. Chem. Phys.* **1976**, *65*, 2925. (b) Pratt, L. R.; Chandler, D. *Ibid.* **1977**, *66*, 147. (c) The analogue of eq 7 for unimolecular isomerizations appears in: Chandler, D. *Ibid.* **1978**, *68*, 2959.

(12) Northrup, S. H.; Hynes, J. T. *J. Chem. Phys.* **1979**, *71*, 871.

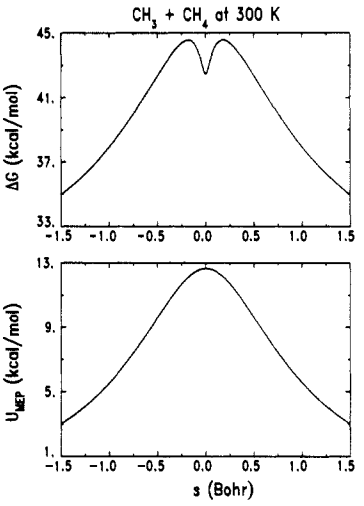

Figure 3. Free energy diagram for the model gas-phase $CH_3 + CH_4$ reaction[7] along the reaction coordinate. The maxima in ΔG are located away from the conventional transition state at $s = 0$, at which the minimum energy path potential energy U_{MEP} is a maximum.

The thermodynamic form of the VTST rate constant indicates that the transition state is located at the point of maximum free energy compared to that of reactants. In contrast, in conventional TST the transition state is located where the potential energy is maximum along the minimum energy path (MEP). But it is now known that the standard TST applied to a heavy–light–heavy reaction system is seriously in error.[7] This can be understood in two ways—dynamic and thermodynamic.

In dynamical terms, the rapid motion of the light particle between its slowly moving heavy neighbors leads to considerable recrossing of the conventional transition-state surface—the surface located at the maximum potential energy of the MEP, i.e., the saddle-point surface. Since TST ignores any such recrossings, the actual rate constant is in consequence much less than the standard TST estimates. The actual reaction bottleneck is located somewhere else.

In the alternate thermodynamic description, a key role is played by vibrational motion *transverse* to the MEP. At large reactant separations, this is the high-frequency HB vibration of frequency ω_{HB}. At the conventional transition-state location where $U \equiv U^{\ddagger}_{c}$, it is the symmetric stretching vibration $\omega^{\ddagger}_{sym}$ in the symmetric H-transfer reaction where A = B. $\omega^{\ddagger}_{sym}$ is usually much less than ω_{HB}, since only heavy particle motion is involved in the former and light H-atom motion dominates the latter. Therefore, since vibrational entropy increases with decreasing frequency, there is an entropy effect that lowers the activation free energy at the conventional transition state. As a consequence, the free energy maximum is shifted away from the conventional transition-state location. This maximum exceeds the TST value, and the rate is accordingly reduced. Truhlar, Garrett, and co-workers[7] have described a VTST technique designed to accurately locate the maximum free energy for H-atom-transfer reactions. Figure 3 shows both the potential energy U_{MEP} along the MEP and the free energy for an illustrative classical model of the gas-phase H transfer between the methyl radical and methane, both without internal structure. At 300 K, the variational TST result for k is a factor of 24.7 less than a standard TST prediction for the same potential surface.[7a] The heavy–light–heavy shifts of the transition state and the free energy are clearly of considerable importance for the rate.

For our calculations of k_{gas}, we will follow Garrett and Truhlar[7a] and calculate the canonical VTST rate constant k_{gas} using a bond energy–bond order (BEBO) method[7,13] to determine the MEP. Here we give only an outline of the procedure; the reader is referred to ref 7a for further details.[14]

The BEBO method assumes the conservation of total bond order $n_{AH}(s) + n_{HB}(s) = 1$ along the collinear MEP characterized by the reaction coordinate s, zeroed at the potential surface saddle point. The bond coordinate–bond order connection is set by the Pauling relations,[7,13] and $U_{MEP}(s)$ is assumed to comprise a Morse potential for each of the AH and HB bonds and an anti-Morse antibonding potential for the AB interaction. Garrett and Truhlar[7a] give the prescription for determining the potential energy for collinear configurations off the MEP, for bent geometries, and for bending vibration energy levels; these are all determined by their prescriptions once $U_{MEP}(s)$ is given. For our solution-phase calculations, we adopt an identical procedure but simply add the solvent contribution $\Delta w_{AB}[r_{AB}(s)]$ to the minimum energy path potential $U_{MEP}(s)$ at any point s along the reaction coordinate. If we denote the *variational* transitional state location by $s^{\ddagger}$ and the solvent density by ρ_s, then the solution rate is

$$k_{soln}(s^{\ddagger},\rho_s) = \sigma_{rx}\frac{k_BT}{h}\frac{Q^{\ddagger}(s^{\ddagger},\rho_s)}{[Q^R(\rho_s)/V]}\exp\left(-\left[\frac{U_{MEP}(s^{\ddagger}) + \Delta w^{\ddagger}_{AB}(s^{\ddagger},\rho_s)}{RT}\right]\right) \quad (8)$$

with the following ingredients. The reactants' partition function is

$$Q^R(\rho_s)/V = (2\pi\mu_{A,HB}k_BT/h^2)^{3/2}Q^R_{vib}(\rho_s)Q^R_{rot} \quad (9)$$

and in principle depends on the solvent through any density-dependent shift in the diatomic reactant vibration frequency ω_{HB}. Since the latter is typically very high ($\approx$3000 cm^{-1}), only a very small solvent shift is expected.[9] We accordingly ignore this in our calculations. The variational transition-state partition function factors into rotational, degenerate bending, and stretching contributions

$$Q^{\ddagger}(s^{\ddagger},\rho_s) = Q^{\ddagger}_{rot}(s^{\ddagger})[Q^{\ddagger}_{bend}(s^{\ddagger},\rho_s)]^2Q^{\ddagger}_{str}[s^{\ddagger},\rho_s] \quad (10)$$

It should be noted that the addition of the solvent contribution Δw_{AB} to U_{MEP} not only modifies the energy along the reaction coordinate s in solution but also slightly modifies the frequencies of the bending and stretching motions perpendicular to s. But as we will see, this only leads to a very small (<10%) shift in $Q^{\ddagger}$ and thus in the rate constant k at liquid solvent densities. The decisive and dominant solvent effect resides in the exponential solvent free energy term $\exp(-\Delta w^{\ddagger}_{AB}/RT)$ in eq 8.

In order to evaluate $\exp(-\Delta w_{AB}/RT)$ for the present atom-transfer problem, we assume that the interactions between the A and B moieties and the solvent molecules are pairwise additive functions of distances between centers of these particles. In this case

$$\exp(-\Delta w_{AB}/RT) = y_{AB}(r_{AB}) \quad (11)$$

where y_{AB} is the indirect pair correlation function[10b,15a] of A and B. Since the structure of nonassociated dense fluids is dominated by short-range repulsions,[10b] we further assume that the interactions of A and B with solvent molecules as well as solvent–solvent interactions may be modeled as hard-sphere repulsions. Since the reacting system is a dilute solution of A and B in solvent s, the quantity required is thus y_{AB} for a pair of hard spheres A and B at infinite dilution in a hard-sphere solvent. This quantity was evaluated by Hsu, Pratt, and Chandler[15a] by extending to infinite dilution the hard-sphere mixture results of Grundke and Henderson.[15b] At the small AB separations that are obtained in the transition-state region, the A and B spheres are overlapped and thus act like overlapping "cavities" with respect to the solvent. In this region, an excellent approximation is (A = B)

$$-\frac{\Delta w_{AB}(r_{AB})}{RT} = \sum_{n=0}^{3} a_n(r_{AB} - \sigma_A)^n/\sigma_A{}^n$$

(13) For a discussion, see: (a) Johnston, H. S. "Gas Phase Reaction Rate Theory"; Ronald Press: New York, 1966. (b) Johnston, H. S.; Parr, C. A. *J. Am. Chem. Soc.* **1963**, *85*, 2544.

(14) There are several misprints in ref 7a: eq 39, 47, 51, 62, and 66.

(15) (a) Pratt, L. R.; Hsu, C. S.; Chandler, D. *J. Chem. Phys.* **1978**, *68*, 4203. (b) Grundke, E. W.; Henderson, D. *Mol. Phys.* **1972**, *24*, 269.

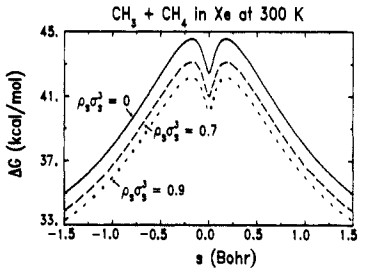

Figure 4. Free energy change ΔG along the minimum energy path (MEP) for the $CH_3 + CH_4$ reaction at 300 K in the gas phase and in Xe solution at two densities.

Table I. Calculated Rate Constant Ratios[a] k_{soln}/k_{gas} for the $CH_3 + CH_4$ Reaction

	Xe		Ar		
$\rho_s\sigma_s^3$	300 K	200 K	200 K	300 K	Ne, 200 K
0.70	11.1	11.1	18.2	18.3	50.0
0.75	15.4	15.3	27.3	27.5	89.3
0.80	22.2	22.0	43.2	43.7	174
0.85	33.7	33.4	73.3	74.3	375
0.90	54.4	53.9	235	137	923
0.95	94.7	94.5	275	281	2670

[a] k_{gas} (200 K) = 3.43 × 10^{-24} cm^3 mol^{-1} s^{-1}; k_{gas} (300 K) = 8.55 × 10^{-20} cm^3 mol^{-1} s^{-1}. A symmetry factor σ_{rx} = 4 has been included.

with σ_A the diameter of A. The four coefficients a_n are obtained from known values of $\exp(-\Delta w_{AB}/RT)$ and its derivatives at $r_{AB} = 0$ and $r_{AB} = \sigma_A$ and consequently depend on σ_A, the solvent diameter σ_s, and the solvent density ρ_s. Since the solvent has the tendency of minimizing the volume of the overlapping solute "cavities", y_{AB} increases rapidly with decreasing r_{AB}.

We stress that the static hard-sphere solvent effects that we will calculate differ from those traditionally[2] viewed as "solvation", i.e., they are not due to any attractive potential forces between the solvent molecules and the reactants and transition state. We will return to this point.

Results

We apply the formalism described above to the model reaction of the transfer of an H atom between methane CH_4 and a methyl radical CH_3 in supercritical rare gas solvents from low up to liquid densities. We ignore for simplicity the complications due to any internal structure of both CH_4 and CH_3. Various potential parameters for the reaction are taken from ref 7 and 13b, identical hard-sphere diameters for CH_3 and CH_4 are taken from ref 16, and hard-sphere solvent diameters are derived from ref 17a. Additive hard-sphere diameters are used throughout this work.

Reaction Rate Constants. Figure 4 compares the calculated gas- and solution-phase free energies $\Delta G^{\ddagger}$ along the reaction coordinate s for Xe solvent ($\sigma_s = \sigma_{Xe}$ = 3.935 Å) at T = 300 K and a high solvent density $\rho_{Xe}\sigma_{Xe}^3 = 0.9$. The solvent static "caging" effect is seen to fairly uniformly lower the free energy in the transition region, i.e., both at the conventional (c) and variational transition states, $s^{\ddagger}_c = 0$ and $s^{\ddagger} = \pm 0.095$ Å, respectively. At the latter, $\Delta w^{\ddagger} \equiv \Delta G^{\ddagger}_{solv} = -2.32$ kcal/mol, and the solution-phase rate constant is enhanced by the considerable factor of 54.4 compared to the gas-phase value.

Figure 4 also includes the free energy calculation at the lower solvent density $\rho_{Xe}\sigma_{Xe}^3 = 0.7$. The free energy lowering is now diminished as expected, and Table I shows that the solvent-induced rate enhancement has dropped to a (still substantial) factor of 22.2. Figure 5 displays the effect as a function of the solvent density.

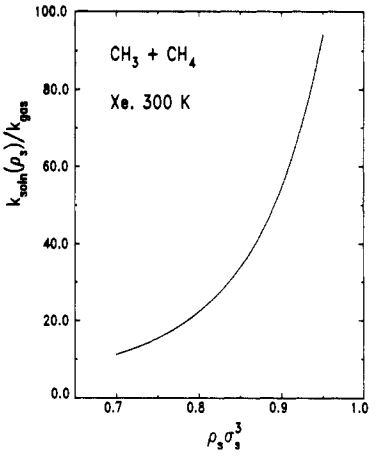

Figure 5. Ratio k_{soln}/k_{gas} of the resolution and gas-phase rate constants vs. reduced solvent density $\rho_s\sigma_s^3$ for the $CH_3 + CH_4$ reaction in Xe at 300 K. The solvent enhancement of the rate constant is apparent.

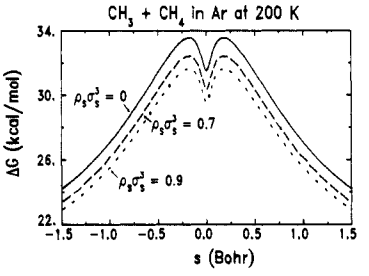

Figure 6. Same as Figure 4 but for the $CH_3 + CH_4$ reaction in Ar at 200 K. The potential energy U_{MEP} in Figure 4 also applies here.

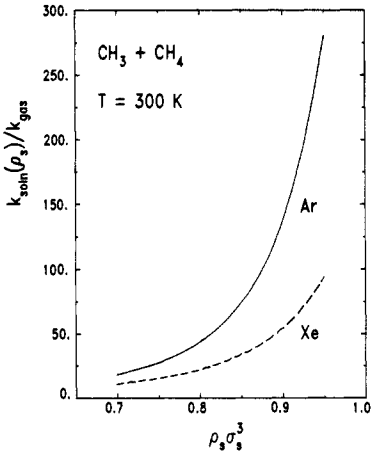

Figure 7. Dependence of the solvent enhancement of the rate constant for $CH_3 + CH_4$ on the solvent identity.

Table I also illustrates the influence of lowering the temperature from 300 to 200 K at a fixed density $\rho_{Xe}\sigma_{Xe}^3 = 0.9$. There is of course a marked lowering of the absolute reaction rate as T is lowered. But there is almost no effect on the solvent acceleration: While there is an approximately linear decrease in the solvent contribution to $\Delta G^{\ddagger}$, there is very little effect on $s^{\ddagger}$ or on k_{soln}/k_{gas}. This feature has its origins in the hard-sphere reactants–solvent interaction model we have adopted. The solvation free energy $\Delta G^{\ddagger}_{solv} \equiv \Delta w^{\ddagger}$ enters k_{soln}/k_{gas} in the form $\Delta G^{\ddagger}_{solv}/RT$, and this turns out to be very nearly temperature-independent (see below). Hard-sphere interaction effects are determined solely by the density and are perforce temperature-independent at fixed density. (We will return to the expected effect of including reactant–solvent attractive forces below.)

The rate enhancement also depends on the *identity* of the solvent at a given temperature T and reduced solvent density $\rho_s\sigma_s^3$. This feature is illustrated by Figure 6 and Table I for Ar solvent at 200 K and $\rho_s\sigma_s^3 = 0.9$. We see that here $\Delta G^{\ddagger}_{solv}$ is more negative, and the solution rate is correspondingly enhanced more compared

(16) Bondi, A. *J. Phys. Chem.* **1964**, *68*, 441.
(17) (a) Verlet, L.; Weis, J.-J. *Phys. Rev. A* **1972**, *2*, 939; *Mol. Phys.* **1972**, *24*, 1013. (b) Weeks, J. D.; Chandler, D.; Andersen, H. C. *J. Chem. Phys.* **1971**, *54*, 523. (c) The use of the hard sphere y_{AB} is consistent with the Weeks–Chandler–Andersen theory for the solvent equation of state, since the same approximation for the solvent–solvent indirect correlation function is used in this theory.

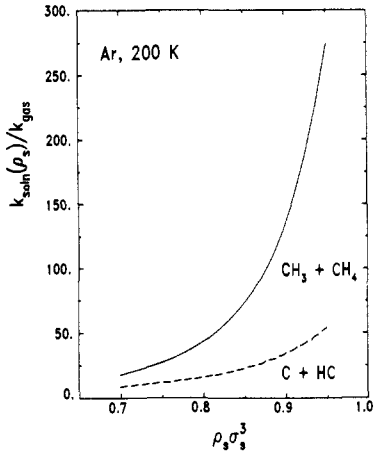

Figure 8. Dependence of the solvent enhancement of the rate constant on the size of the A and B flanking groups in the AH + B reaction in Ar solvent at 200 K.

to the Xe case at the same temperature and reduced density (cf. Table I). The origin of this effect is quite simple, and analogous trends have been predicted for the effects of solvent size on conformational equilibria.[11a] The solvent "pressure" enhancing the generalized transition-state probability is greater for the smaller (σ_s = 3.40 Å) Ar solvent atoms compared to the larger Xe atoms. Packing around the transition-state structure is easier for the smaller Ar atoms and the actual solvent density ρ_s is larger. This important feature is strongly reinforced in Figure 7, which displays the considerable acceleration of the reaction in Ar compared to Xe solvent. Indeed, at $\rho_s\sigma_s^3 = 0.90$ and T = 200 K, k_{soln}/k_{gas} = 54 in Xe, while k_{soln}/k_{gas} = 135 in Ar.

We can pursue this point with a further calculation in Ne solvent at 200 K. The hard-sphere diameter σ_s for Ne is approximately 2.59 Å, which is noticeably smaller than the methyl diameter of 3.65 Å. The rate enhancement should thus increase, since the smaller Ne solvent can very effectively pack around the transition state. Indeed, Table I shows that at the highest solvent densities $\rho_s\sigma_s^3$ = 0.9–0.95, k_{soln} is about *3* orders of magnitude greater than k_{gas}! We believe that this basic trend with decreasing solvent size is correct, but the predicted numbers should be viewed with some caution. For with a small solvent atom, our hard-sphere interaction model involving *structureless* methyl groups should begin to break down. Any "penetration" ability of the solvent molecules into the transition-state structure will clearly reduce the enhancement of the solution rate constant compared to a structureless reactant–solvent interaction model. This expectation is supported by the work on solvent shifts of the *n*-butane trans–gauche equilibrium constant in hard-sphere and more highly structured solvents.[15a]

Finally, the solution-phase rate enhancement depends quite markedly on the *size* of the A and HB reacting groups. Figure 8 shows our results for the model reaction in which the CH_3 and CH_4 moities are replaced by the smaller bare C atoms, with all intramolecular potentials kept the same. But now the solvent interacts with a smaller hard core (σ_C = 3.32 Å) vs. $\sigma_{CH_3} = \sigma_{CH_4}$ = 3.65 Å. In Ar solvent at 200 K and $\rho_s\sigma_s^3$ = 0.9, the rate enhancement drops by about a factor of 5 on replacing CH_3 and CH_4 by C atoms. The smaller cavity presented to the solvent by the C atoms is the origin of the effect.

The CHC reaction example also allows us to simply "dissect" the reaction rate constant into its components to emphasize several important points. The ratio of solution- to gas-phase rates is, in detail

$$\frac{k_{soln}(s^\ddagger,\rho_s)}{k_{gas}(s^\ddagger)} = \frac{Q^\ddagger(s^\ddagger,\rho_s)}{Q^\ddagger(s^\ddagger,0)} \exp\left[-\frac{\Delta w^\ddagger}{RT}(s^\ddagger,\rho_s)\right] \quad (12)$$

in which the partition functions factor into rotational, bend, and stretch contributions

$$Q^\ddagger(s^\ddagger) = Q^\ddagger_{rot}(s^\ddagger)[Q^\ddagger_{bend}(s^\ddagger)]^2 Q^\ddagger_{str}(s^\ddagger) \quad (13)$$

Table II. Ingredients of the Rate Constant for the Model C + HC Reaction at 200 K in Ar at $\rho_s\sigma_s^3 = 0.9$[a]

$R^\ddagger_{bend}$	$R^\ddagger_{rot}$	$R^\ddagger_{str}$	$R^\ddagger$	$e^{-\Delta w^\ddagger/RT}$	$e^{-\Delta w^{\ddagger,c}/RT}$
1.085	1	1.000	1.177	30.87	32.62

[a] $R^\ddagger$ denotes the solution- to gas-phase partition function ratios $Q^\ddagger(\rho_s)/Q^\ddagger(\rho_s = 0)$ for the bend, rotation, stretch, and overall product (cf. eq 13). The notation $\Delta w^{\ddagger,c}$ distinguishes the conventional transition-state value from the variational result $\Delta w^\ddagger$.

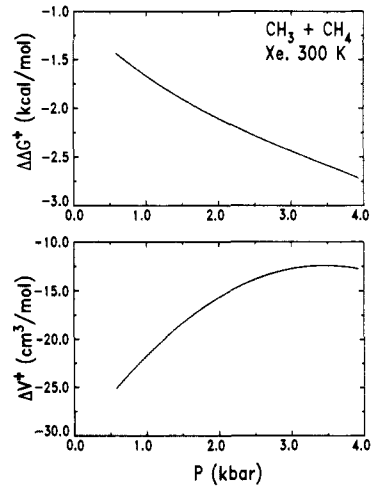

Figure 9. Upper panel: Solvation free energy of activation $\Delta\Delta G^\ddagger$ for the $CH_3 + CH_4$ reaction at 300 K as a function of the solvent Xe pressure. Lower panel: The reaction volume of activation $\Delta V^\ddagger$. This quantity is obtained from a third-order polynomial fit in p to $\Delta\Delta G^\ddagger$.

The variational transition state is located at $s = s^\ddagger = \pm 0.097$ Å where the CH bond order is n_{CH} = 0.372. (The conventional transition state is at s = 0, where n_{CH} = 0.5.) Table II summarizes the various ingredients of the rates at 200 K for Ar solvent.

First, we see that—as alluded to above—the temperature dependence of k_{soln}/k_{gas} arising solely from the partition function factors [i.e., exclusive of $\exp(-\Delta w^\ddagger/RT)$] is very weak. Second, the solvent density dependence of the partition functions' contribution to the rate is small; to an excellent approximation one can focus exclusively on the solvent contribution $\exp[-\Delta w^\ddagger/RT]$ as we have done throughout. A related point is that the pattern of the shifts in the partition functions on going from s = 0 to $s = s^\ddagger$ is *not* at all perturbed by solvent effects. Finally, the previously noted very slow variation of the solvent contribution to the free energy, Δw, throughout the entire transition-state region is quantified here. The exponentially amplified effect on $\exp(-\Delta w/RT)$ on moving from s = 0 to $s = s^\ddagger$ is only about 5% and is completely negligible.

Thermodynamic Parameters. We now turn our attention to several convenient thermodynamic probes of the solution rate. The first of these is the activation volume $\Delta V^\ddagger$ defined by the pressure derivative of the rate constant ratio

$$-RT[(\partial \ln k_{soln}/k_{gas})/\partial p]_T = \partial \Delta w^\ddagger/\partial p|_T = \Delta V^\ddagger \quad (14)$$

(Recall that all our rate constants refer to concentration rate laws and that k_{gas} is pressure-independent by definition.) In contrast to the solvent free energy term $\Delta w^\ddagger$, the solvent pressure p is a very sensitive function of the solvent–solvent attractive forces and cannot possibly be realistically modeled in hard-sphere terms. We therefore adopt a realistic Lennard-Jones (LJ) potential model for the solvent–solvent interactions to compute the pressure. Verlet and Weis[17a] have developed a convenient analytical method, based on the Weeks–Chandler–Andersen[17b] theory, for calculating the compressibility factor $Z = p/\rho_s k_B T$ for LJ fluids and have given a set of LJ parameters that leads to good agreement with experiment for the rare gases. We use these authors' expression for Z, which then gives us the solvent pressure as a function of temperature and density.[17c]

Figures 9 and 10 display our results for the CH_3–CH_4 reaction in Ar and Xe solvents. There are several important features to

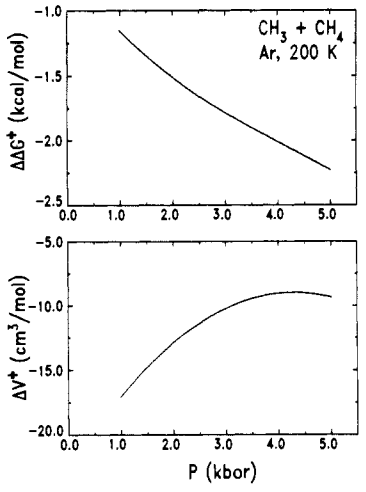

Figure 10. Same as Figure 9 but for Ar solvent. Note the contrasting magnitudes of $\Delta V^{\ddagger}$ here and in Figure 9 for the different solvents.

note. First, $\Delta\Delta G^{\ddagger} \equiv \Delta G^{\ddagger}_{soln} - \Delta G^{\ddagger}_{gas}$ is monotonically more negative with increasing pressure p: the solvent density stabilization of the variational transition state progressively increases. Second, the activation volume $\Delta V^{\ddagger}$ is a *strong* function of the solvent pressure, even within the range of very high liquid-state densities. This marked variation arises from the different rates at which the increasing density increases k on the one hand and increases the pressure p on the other. This striking feature warrants a pause for further discussion.

It is often thought[1,2] that for nonpolar, nonionic reactants, the activation volume is, in significant part, a direct reflection of the *geometric* decrease of the volume of the transition state $V^{\ddagger}$ compared to the volume V^{R} of the reactants, such that the identification $\Delta V^{\ddagger} = V^{\ddagger} - V^{R} \equiv \Delta V^{\ddagger}_{geom}$ is posited. We find absolutely no support for this idea. First and foremost, $\Delta V^{\ddagger}_{geom}$ is by definition a constant for a given reaction. As such, $\Delta V^{\ddagger}_{geom}$ will not vary with p or solvent; we find that $\Delta V^{\ddagger}$ clearly and markedly varies. Second, we find little correlation between the magnitudes of $\Delta V^{\ddagger}$ and $\Delta V^{\ddagger}_{geom}$, even in the very high-pressure regime where $\Delta V^{\ddagger}$ has its least variation. Let us stress this point. If we model the transition state in a traditional way as two overlapping spheres, then it is a simple exercise in geometry to show that $\Delta V^{\ddagger}_{geom}$ is just the negative of the overlap volume of those spheres. This works out to be

$$\Delta V^{\ddagger}_{geom} = -\frac{2\pi N_0}{3}\left(\sigma_A - \frac{1}{2}r^{\ddagger}_{AB}\right)^2\left(2\sigma_A + \frac{1}{2}r^{\ddagger}_{AB}\right)$$

Here σ_A is the diameter of molecule A and $r^{\ddagger}_{AB}$ is the separation between the outer A and B group centers at $s^{\ddagger}$. For the CH_3 + CH_4 case, $\sigma_A = 3.65$ Å and $r^{\ddagger}_{AB} = 2.56$ Å. This gives $\Delta V^{\ddagger}_{geom} = -60.8$ cm^3/mol. Comparison with Figures 9 and 10 shows that $\Delta V^{\ddagger}_{geom}$ has no discernable direct relevance for the rate problem.[18]

Certainly, experimental pressure-dependent activation volumes are well-known, and they are usually interpreted in terms of differing "compressibilities" of the reactants and the transition state.[19] The variation of $\Delta V^{\ddagger}$ observed here is not due to any such compressibility effects, since we find that the AB separation at the transition state is negligibly pressure-dependent. Rather, the variation of $\Delta V^{\ddagger}$ with p arises from the changing solvent packing about the transition state.

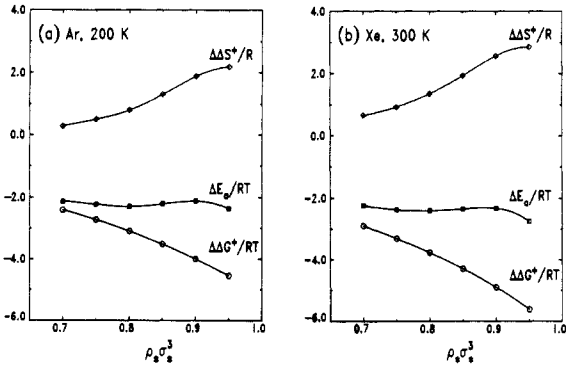

Figure 11. Solvation activation parameters vs. reduced solvent density for the CH_3 + CH_4 reaction in (a) Ar at 200 K and (b) Xe at 300 K.

Finally, we examine the thermodynamic "transfer" functions[20] associated with the difference of the reaction activation parameters in solution and in the gas phase. The transfer activation free energy

$$\Delta\Delta G^{\ddagger} = \Delta G^{\ddagger}_{soln} - \Delta G^{\ddagger}_{gas} = \Delta w^{\ddagger} \quad (15)$$

is determined solely by the solvent mean potential and is thus a solvation free energy of activation. With eq 14 and 15, some straightforward thermodynamic manipulation, and one mild assumption,[21] it is easy to show that the transfer activation enthalpy is given by

$$\Delta\Delta H^{\ddagger} = \Delta H^{\ddagger}_{soln} - \Delta H^{\ddagger}_{gas} = -T^2[\partial(\Delta w^{\ddagger}/T)/\partial T]_p = T\Delta V^{\ddagger}(\partial p/\partial T)_p \quad (16)$$

and that the transfer activation entropy is

$$\Delta\Delta S^{\ddagger} = \Delta S^{\ddagger}_{soln} - \Delta S^{\ddagger}_{gas} = -\partial(\Delta w^{\ddagger}/\partial T)_p = -\Delta w^{\ddagger}/T + \Delta V^{\ddagger}(\partial p/\partial T)_p \quad (17)$$

These transfer functions can be directly connected to the experimental Arrhenius factors for the reaction. The experimental activation energy in a given phase is given by[3a]

$$E_a = RT^2\partial \ln k/\partial T]_p = \Delta H^{\ddagger} + RT \quad (18)$$

and the preexponential A factor in the standard Arrhenius form $k = Ae^{-E_a/RT}$ is

$$A = (ek_BT/h)K^{\circ}e^{\Delta S^{\ddagger}/R} \quad (19)$$

Thus $\Delta\Delta H^{\ddagger}$ gives the shift in activation energy between phases

$$\Delta\Delta H^{\ddagger} = \Delta E_a \quad (20)$$

i.e., the activation energy shift is just the solvation enthalpy of activation, and the phase change in the A factor is determined by the transfer activation entropy $\Delta\Delta S^{\ddagger}$, i.e., the solvation entropy of activation

$$A_{soln}/A_{gas} = \exp[\Delta\Delta S^{\ddagger}/R] \quad (21)$$

We can calculate all these thermodynamic transfer functions with the values of k_{soln}/k_{gas} and $\Delta V^{\ddagger}$ that we have previously obtained and the numerical evaluation of $(\partial p/\partial T)_p$ for the appropriate LJ fluid. The results are shown in Figure 11 for CH_3 + CH_4 in Xe at 300 K and in Ar at 200 K. There are several points to note. First, the activation energy shift $\Delta E_a = \Delta\Delta H^{\ddagger}$ is approximately *constant* with density, with a value in the range -2 to $-2.5RT$.[22] In contrast, many approximate theories assume

(18) (a) A related comment has been made in connection with the association equilibrium constants by: Chandler, D. *Discuss. Faraday Soc.* **1978**, *66*, 184. (b) The zero density asymptote $\Delta V^{\ddagger}_0 = \lim_{\rho_s\to 0} \Delta V^{\ddagger}$ can be found analytically from the Percus–Yevick equation for hard-sphere mixtures with the results in: Lebowitz, J. L. *Phys. Rev.* **1964**, *133*, A895. The result is $\Delta V^{\ddagger}_0 = -N_0\pi[(\sigma^{\ddagger} + \sigma_s)^3/6 - [(\sigma^{\ddagger} + \sigma_s)^2 r^{\ddagger}/4] + (r^{\ddagger 3}/12)]$, which is -53 cm^3/mol in Ar and -75 cm^3/mol in Xe. Note that $\Delta V^{\ddagger}_0$ is solvent-dependent.

(19) (a) Kohnstam, G. *Prog. React. Kinet.* **1970**, *5*, 335. (b) Whalley, E. *Adv. Phys. Org. Chem.* **1964**, *2*, 93. (c) Le Noble, W. J. *Ibid.* **1965**, *5*, 207. (d) Asano, T.; Le Noble, W. J. *Chem. Rev.* **1978**, *78*, 407.

(20) Leffler, J. E.; Grunwald, E. "Rates and Equilibria of Organic Reactions"; Wiley: New York, 1963.

(21) We have assumed that $\Delta w^{\ddagger}/RT$ is independent of temperature at fixed density. This is exact[10] for hard-sphere interactions. Note however that all derivatives involving pressure are evaluated for the appropriate LJ pressure rather than the pressure of a hard-sphere solvent.

no solvent effect on the activation energy. Second, the transfer activation free energy $\Delta\Delta G^{\ddagger}$ decreases by about a factor of two in the density range $\rho_s\sigma_s^3 = 0.7$–0.95. Third—and as a consequence, the *variation* of k_{soln}/k_{gas} over this density and pressure range is determined by the transfer activation entropy $\Delta\Delta S^{\ddagger}$, which increases significantly in this range (by about a factor of 9 for Xe and a factor of 5 for Ar). Indeed, at the very highest solvent densities and pressures, the $\Delta\Delta S^{\ddagger}$ component tends to dominate $\Delta\Delta G^{\ddagger}$, i.e., $T\Delta\Delta S^{\ddagger} \approx -2\Delta\Delta H^{\ddagger}$. Equivalently, the density and pressure variation of k_{soln}/k_{gas} is here determined by the preexponential A values. The other side of this coin is that, from eq 16–18, at the highest solvent densities and pressures, the transfer activation entropy is in the main determined by the solvent free energy contribution $-\Delta w^{\ddagger}/T$. Thus in this regime, we can approximately identify the solvent free energy acceleration of the solution rate with the increased entropy associated with the solvent packing about the transition-state structure. It is also worth noting that we find no "compensation" effect[20] over the entire density range; i.e., both enthalpic and entropic contributions lower the free energy.

At this point, we need to stress that the activation volume $\Delta V^{\ddagger}$ is defined by eq 14 in terms of the pressure derivative of the concentration rate constant. It is this definition (and the analogous definitions above for $\Delta\Delta G^{\ddagger}$, $\Delta\Delta H^{\ddagger}$, and $\Delta\Delta S^{\ddagger}$) that isolated the solvent effects on thermodynamic rate parameters. (Note that all are zero if $\Delta w^{\ddagger} = 0$.)

Now it is correctly pointed out by many authors[19,23] that e.g., the pressure derivative of a concentration rate constant involves both a certain volume term and a compressibility term. As applied to k_{soln}/k_{gas}, one can correctly write (k_{gas} as defined in eq 3 is completely pressure-independent)

$$-RT^2\,\partial \ln (k_{soln}/k_{gas})/\partial p|_T = \Delta\bar{V}^{\ddagger} + RT\kappa_s \qquad (22)$$

where $\Delta\bar{V}^{\ddagger} = \bar{V}^{\ddagger} - \bar{V}_A - \bar{V}_{HB}$ is the difference in partial molar volumes and κ_s is the solvent compressibility $\kappa_s = \partial \ln \rho_s/\partial p_s|_T$. From this it would appear that eq 22 contains an unwanted compressibility term and that one should instead consider rate constants in terms of volume-independent mole fractions or molal concentrations. But this is *not* the case if one wishes to exclusively expose solvent effects. There is evidently a hidden $-RT\kappa_s$ term in $\Delta\bar{V}^{\ddagger}$ canceling the explicit $RT\kappa_s$ contribution.[24] Both eq 22 and 14 are valid, but $\Delta\bar{V}^{\ddagger}$ is not the desired indicator of the solvent effect on k. It is instead $\Delta V^{\ddagger}$ given by eq 14 since that quantity is determined solely by $\Delta w^{\ddagger}$. Analogous remarks apply to $\Delta\Delta H^{\ddagger}$ and $\Delta\Delta S^{\ddagger}$.[24]

Estimation for Loose Transition States. The major reason we have found such large solvent enhancement in our model H-atom-transfer studies is the "tight" character of the transition state. The relatively small separation between the terminal group centers, e.g., 2.56 Å in the $CH_3 + CH_4$ example, means that the van der Waals spheres of the CH_3 and CH_4 terminal groups with $\sigma = 3.65$ Å are considerably overlapped. Thus the cavity presented to the solvent is subject to large entropic solvent forces.

The magnitude of this effect, and thus the solvent enhancement of the rate, will decline as the transition state becomes progressively more "loose". As the separation of the terminal group centers increases toward the sum of their hard-sphere radii, the overlap diminishes and so do the solvent mean potential forces. Figure 12 illustrates this important effect for an artificial series of $CH_3 + CH_4$ reactions in which the transition state CH_3–CH_4 separation $r^{\ddagger}$ is progressively lengthened. It is seen that the solvent rate enhancement drops fairly precipitously. At the largest $r^{\ddagger}$ values

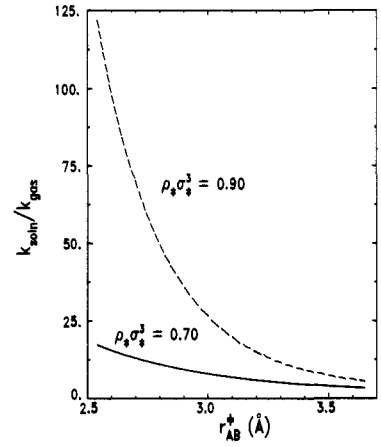

Figure 12. Suppression of the solvent rate constant enhancement for loose transition states. As the end group separation $r^{\ddagger}_{AB}$ in the $CH_3 + CH_4$ transition state is artificially lengthened, the rate constant ratio k_{soln}/k_{gas} declines at a rate determined by the solvent density (Ar, 200 K).

$\approx \sigma_{CH_3}$, the enhancement is reduced to only a factor of ≈ 5. This in fact is just the order of magnitude of the radial distribution at contact,[10,12] which is the relevant solvent enhancement factor for simple collisional nonactivated problems in solution.[12] We conclude the marked solvent atom transfer rate enhancements will require fairly *tight* transition-state structures to be seen and that H-atom transfers are attractive candidates in this connection.

Discussion. The methyl–methane H abstraction reaction has been studied in the gas phase via assorted isotopic substitutions,[25] but we are unaware of any solution studies available for comparison with our results.

It would therefore be of interest if these rates could be measured in rare gas solutions. In this connection, we need to consider two features ignored in the present treatment. First, there is evidence that the H atom transfer in $CH_3 + CH_4$ proceeds predominantly by a tunneling mechanism in the gas phase,[7a,26,27] and one should be concerned whether this is heavily influenced by the solvent.[27]

Second, we have ignored in the calculation of $\Delta G^{\ddagger}_{soln}$ any contribution of the reaction system–solvent attractive forces. In view of Figure 2, this is equivalent to assuming that, e.g., attractive dispersion forces for separated reactants are nearly the same as in the transition state.[28] In fact, due to the more compact nature of the transition state compared to the reactants, one expects a certain decrease in these forces on passing to the transition state. This may lead either to an enhancement or a suppression of k_{soln}, depending on the relative strengths of solvent–solvent and solute–solvent interactions.[29] However, any attractive force solvation for CH_4 and CH_3 should be rather weak, and we do not expect a pronounced reduction of the solvent enhancement of k_{soln}/k_{gas}.

Strong and specific attractive solvent forces have been implicated in some H-atom abstractions. For example, H-atom abstractions from OH bonds are thought to reflect strong hydrogen bonding solvation effects in which the reactants are typically stabilized,[30] and solvent complexation of chlorine atoms in the solution-phase reactions of Cl with CH bonds has been discussed.[31]

(22) The "internal pressure" p_i for a solvent is $p_i = T(\partial p/\partial T)_\rho - p$ [See, e.g., Dack, M. *Chem. Soc. Rev.* **1975**, *4*, 211]. Thus by eq 20 and 21, the activation energy shift is $\Delta E_s = [p_i - p]\Delta V^{\ddagger}$. For liquid solvents in which $p_i \gg p$, this will simplify. However, we find that $p_i \approx 1$–2 kbar for Ar at 200 K and Xe at 300 K, so that the internal pressure contribution does not dominate the activation energy shift in these solvents.

(23) Hamann, S. D.; Le Noble, W. J. *J. Chem. Educ.* **1984**, *61*, 659.

(24) This point has been made in connection with equilibrium constants in Ben-Naim, A. *J. Phys. Chem.* **1978**, *82*, 792 (see also ref 5b). A more detailed discussion for rates is in preparation: Ladanyi, B. M.; Hynes, J. T. unpublished.

(25) (a) Dainton, F. S.; Ivin, K. J.; Wilinson, F. *Trans. Faraday Soc.* **1959**, *55*, 929. (b) Creak, G. A.; Dainton, F. S.; Ivin, K. J. *Ibid.* **1962**, *58*, 326.

(26) Babamov, V. K.; Marcus, R. A. *J. Chem. Phys.* **1978**, *74*, 1790.

(27) Ali, D. P.; Hynes, J. T. *J. Chem. Phys.*, submitted.

(28) Note that this is not the approximation that there are no dispersion force interactions of the solvent with the reactants and the transition state.

(29) When solute–solvent dispersion forces are larger than solvent–solvent ones, their effects on Δw_{AB} could be analogous to those found in the calculation of the effective vibrational potential for Br_2 in Ar (Nordholm, S.; Freaser, B. C.; Hamer, N. D.; Jolly, D. L. *Chem. Phys.* **1980**, *47*, 347). The situation is complicated by the fact that the predicted effective potential changes substantially when the Br–Br distance dependence of the strength of Br–Ar dispersion forces is taken into account (Pratt, L. R.; Chandler, D. *J. Chem. Phys.* **1980**, *72*, 4045).

(30) For a review, see: Simonyi, M.; Tüdös, F. *Adv. Phys. Org. Chem.* **1971**, *9*, 127.

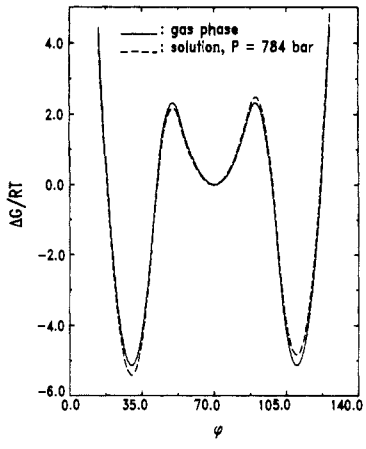

Figure 13. Reduced free energy $\Delta G/RT$ vs. dihedral angle φ for 1,1'-binaphthyl isomerization in benzene solution at 293 K. The corresponding result at $p = 1$ bar (not shown) is very close to that at $p = 784$ bar.

Since such attractive force effects are in *competition* with static solvent caging effects of the sort we have discussed, these attractive forces are presumably even *stronger* than has been thought. In any event, it would be of interest to attempt the study of these reactions in inert gas solvents to help sort out opposing solvent effects on the rate constants.

Finally, concerning H-atom transfers of the methyl–methane variety, H-atom abstraction from higher alkanes than methane has been studied in the gas phase.[32] We are unaware of any corresponding studies in solution. We would expect solvent caging effects in such cases to progressively diminish: increasingly nonspherical alkane reactants should lead to solvent packing whose entropic force is increasingly less directed along the relevant methyl–alkane axis in the transition state.

Isomerizations

For simple geometric isomerization reactions in solution, transition states are typically very "loose"; i.e., groups rotating about a bond usually do not overlap each other. As a consequence, static solvent effects[15a,33] will be relatively minor compared to the atom-transfer case. In order to estimate the magnitude of this effect, we consider the photoisomerization of 1,1'-binaphthyl dissolved in benzene at 293 K, which was a subject of a recent experimental study.[34a] We adopt simple models of solute and solvent structures: naphthyl groups and solvent molecules are both represented as hard spheres. The naphthyl group diameter, $\sigma_{NA} = 4.228$ Å, is chosen so the naphthyl groups are in contact but are not overlapped at their minimum distance of approach, corresponding to the dihedral angle $\varphi = 0$. For benzene we choose the diameter $\sigma_s = 5.12$ Å, obtained from diffusion constant measurements.[34b] The McCaskill–Gilbert gas-phase naphthyl–naphthyl potential[34c] is used in these calculations. In Figure 13 we compare the results for the mean potential in benzene under pressure of 784 bar, corresponding to $\rho_s\sigma_s^3 = 0.945$,[34b] to the gas-phase potential. The two potentials are seen to differ very little. The small change in $\Delta\Delta G[r(\varphi)]$ is due to the fact that the naphthyl–naphthyl distance, r, is outside the overlap region and that it changes only from $1.0\sigma_{NA}$ to $1.1\sigma_{NA}$ over the entire range of φ depicted in Figure 13. As a consequence, the effect of the solvent on the TST rate is quite small. For the isomerization to cis ($\varphi = 70° \rightarrow \varphi = 30°$), we calculate that $k_{soln}/k_{gas} = 1.16$ and

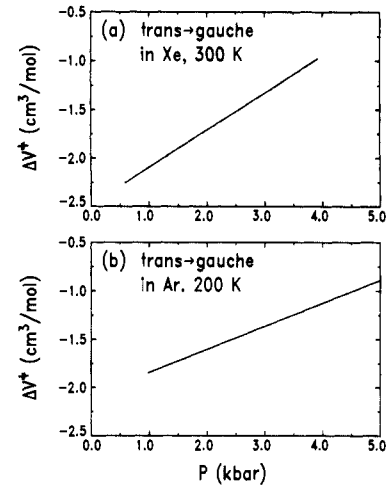

Figure 14. Volume of activation $\Delta V^{\ddagger}$ vs. solvent pressure p in (a) Xe solvent at 300 K and (b) Ar solvent at 200 K. Values are obtained by second-order polynomial in p fits to $\Delta\Delta G^{\ddagger}$.

for the isomerization to trans ($\varphi = 70° \rightarrow \varphi = 90°$), $k_{soln}/k_{gas} = 0.86$. The barrier in the isomerization to trans is increased since the transition state corresponds to a larger $r(\varphi)$ than the reactant well and since in this region the naphthyl–naphthyl indirect correlation function decreases toward the minimum located between first- and second-neighbor shells.

Such relatively minor solvent effects are also found in other isomerization rate studies[33] and lend support to the simplified treatments of TST predictions that indicate that $k_{soln}/k_{gas} \approx 1$ for unimolecular isomerizations.[1-3] Nonetheless, there can be a very important static solvent effect revealed if we examine $\Delta V^{\ddagger}$.

We illustrate this point for a different isomerization. We adopt the two-site model of Pratt et al[15a] for the *n*-butane isomerization and calculate $\Delta V^{\ddagger}$ for the trans to gauche isomerization using

$$k_{soln}/k_{gas} = e^{-\Delta\Delta G^{\ddagger}/RT} = e^{-\Delta w^{\ddagger}(r^{\ddagger})/RT} \quad (23)$$

Here r is the separation of the rotating methyl group centers

$$r = L[\tfrac{1}{2}\cos\varphi\sin^2(\pi-\theta) + \tfrac{3}{2} + 2\cos(\pi-\theta) + \tfrac{1}{2}\cos^2(\pi-\theta)]^{1/2} \quad (24)$$

in which L = 1.54 Å is the CC bond length, $\theta = 112°$ is the CCC bond angle, and φ is the dihedral angle [$\varphi = 0$ for trans and $\varphi = 57°$ for the barrier].

Figure 14 shows the $\Delta V^{\ddagger}$ values obtained for the butane isomerization in Ar at 200 K and in Xe at 300 K. Two key points are apparent. First, $\Delta V^{\ddagger}$ depends on the solvent. Second, $\Delta V^{\ddagger}$ varies approximately linearly with the pressure in the range studied. This last feature has particular relevance for pressure studies of solution isomerizations designed to isolate *dynamic* solvent effects on the reaction rate. Any significant variation in $\Delta V^{\ddagger}$ such as apparent in Figure 14 will lead to a pressure variation in the TST rate that is different from that predicted with an assumed *constant* $\Delta V^{\ddagger}$ value. This leads to the possibility that pressure variations in k associated with a variation in $\Delta V^{\ddagger}$ would then be incorrectly identified as dynamic solvent effects. A discussion of this possibility for the cyclohexane inversion[35] is presented elsewhere.[36]

Conclusions

Extensive calculations on the model H-atom transfer between methyl radical and methane indicate that significant static solvent caging enhancement of rate constants in rare gas solution is likely. Activation volumes vary strongly with pressure and solvent and are not directly related to standard geometric ideas about the transition state. Such solvent enhancements are likely to be

(31) For a review, see: Huyser, E. S. *Adv. Free-Radical Chem.* **1965**, *1*, 77.
(32) Jackson, W. M.; McNesby, J. R.; Darwent, B. deB. *J. Chem. Phys.* **1963**, *37*, 1610.
(33) (a) Rebertus, D. W.; Berne, B. J.; Chandler, D. *J. Chem. Phys.* **1979**, *70*, 3395. (b) Ladanyi, B. M.; Evans, G. T. *Ibid.* **1983**, *79*, 944. (c) Jorgensen, W. L.; Binning, R. C., Jr.; Bigot, B. *J. Am. Chem. Soc.* **1981**, *103*, 4393.
(34) (a) Shank, C. V.; Ippen, E. P.; Teschke, O.; Eisenthal, K. B. *J. Chem. Phys.* **1977**, *67*, 5547. (b) Parkhurst, H. J.; Jonas, J. *J. Chem. Phys.* **1975**, *63*, 2705. (c) McCaskill, J.; Gilbert, R. *Chem. Phys.* **1979**, *44*, 389.
(35) Hasha, D. L.; Eguchi, T.; Jonas, J. *J. Am. Chem. Soc.* **1982**, *104*, 2290.
(36) Zawadzki, A. G.; Hynes, J. T. *J. Chem. Phys.*, submitted.

maximal for tight transition-state reactions such as the CH_3 + CH_4 system and to diminish as the transition state becomes more loose and the reacting moities become more complex. Static solvent caging effects are much less pronounced in typical isomerizations. Nonetheless, pressure variation of the activation volume can play an important role in the elucidation of dynamic solvent effects on rates.

Acknowledgment. B.M.L. acknowledges support of this work by NSF Grant CHE84-05165. Computational work was supported by NIH Grant GM27945. Acknowledgment is made by J.T.H. to the Donors of the Petroleum Research Foundation, administered by the American Chemical Society, for partial support of this work. J.T.H. also acknowledges support by NSF Grants CHE81-13240 and CHE84-19830.

Substituent Effects on Neutral and Ionized C=C and C=O Double Bonds and Their Implications for the Stability Order of Keto/Enol Tautomers

Nikolaus Heinrich,* Wolfram Koch, Gernot Frenking,*† and Helmut Schwarz*

Contribution from the Institut für Organische Chemie der Technischen Universität Berlin. D-1000 Berlin 12, West Germany. *Received June 27, 1985*

Abstract: By using ab initio molecular orbital (MO) calculations substituent effects on monosubstituted neutral as well as cationic ethylene and formaldehyde are studied. The relative stabilizations caused by substitution have been evaluated by means of isodesmic reactions employing a complete "first row sweep". The so-obtained results have been used to investigate the relative stabilizations of simple, substituted neutral and cationic keto/enol pairs. π-donating and -accepting as well as σ-accepting substituents were found to stabilize the neutral C=C bond thermochemically. The C=O double bond is highly stabilized by π-donating and σ-accepting substituents, and the stabilization effects are much larger compared to those found for the corresponding C=C double bond systems. Substantial stabilization is provided by a strong polarization of the double bond. Substituents which are able to reinforce an already existing bond polarization are stabilizing most efficiently. In the cationic species, the ability of the substituent to donate negative charge, thereby compensating the electron deficiency caused by ionization, is found to be of prime importance. Both σ- and π-donors provide substantial stabilization. The relative stabilizations for C=O double bond containing cationic species are smaller for π-donating groups and larger for σ-donors compared to the corresponding cationic ethylene derivatives. These findings also apply for neutral and ionized acetaldehyde and vinyl alcohol derivatives. The effect on the respective keto/enol energy differences is discussed.

It is well-known that simple noncrowded neutral ketones, aldehydes, and carboxylic acids are, in general, thermochemically and kinetically more stable than their corresponding enol forms.[1] However, for the cation radicals of keto/enol pairs a reversal of the stability order is observed. The enol form usually turns out to be the more stable tautomer as shown by both experiment[2] and theory.[3] The energy difference between neutral and charged keto/enol pairs is highly dependent upon the electronic properties of the substituent attached directly to the C=O or C=C double bond, respectively. Obviously, the understanding of substituent effect on C=C and C=O double bonds in neutral or charged molecules is a prerequisite for explaining the remarkable effects observed for the keto/enol pairs. In this paper we report on our results of ab initio molecular orbital (MO) calculations on monosubstituted neutral and cationic ethylene and formaldehyde derivatives in order to rationalize the effect of a substituent in terms of its electronic properties. The effect of substituents located at the α-carbon atom of neutral and cationic vinyl alcohol and acetaldehyde are analyzed in a systematic way[4] by means of isodesmic reactions.[5] Additional work concerning the substituent effects on the transition states for the interconversions of keto/enol tautomers, which are highly affected by the nature of a substituent, is in progress and will be published elsewhere.[6,7] For a thorough study of substituent effects we employed a complete "first row sweep", and the substituents that were chosen, i.e., F, OH, NH_2, CH_3, BH_2, and BeH, encompass a wide range of electronic properties.[4] F is a strong σ-acceptor and a weak π-donor; both OH and NH_2 are strong π-donors but weaker σ-acceptors. CH_3 exerts much milder electronic effects, being capable of acting either as a π-donor or π-acceptor and, additionally, as a weak σ-donor.

† Present address: SRI International, Menlo Park, CA 94025.

(1) For leading references, see: (a) Forsen, S.; Nilsson, M. In "The Carbonyl Group, II"; Patai, S., Ed.; Wiley Interscience: New York, 1970. (b) Holmes, J. L.; Terlouw, J. K.; Lossing, F. P. *J. Phys. Chem.* **1976**, *80*, 2860. (c) Bouma, W. J.; Poppinger, D.; Radom, L. *J. Am. Chem. Soc.* **1977**, *99*, 6443. (d) Pollack, S. K.; Hehre, W. J. *Ibid.* **1977**, *99*, 4845. (e) Bell, R. P.; Smith, P. W. *J. Chem. Soc., Perkin Trans. 2* **1977**, *7*, 241. (f) Noack, W. E. *Theor. Chim. Acta* **1979**, *53*, 101. (g) Hart, H. *Chem. Rev.* **1979**, *79*, 515. (h) Dubois, J.-E.; El-Alaoui, M.; Toullec, J. *J. Am. Chem. Soc.* **1981**, *103*, 5393. (i) Chiang, Y.; Kresge, A. J.; Walsh, P. A. *Ibid.* **1982**, *104*, 6122. (j) Toullec, J. *Adv. Phys. Org. Chem.* **1982**, *18*, 1. However, the stabilities of both neutral and ionic crowded keto/enol pairs differ strongly from that observed for simple systems, see: (k) Biali, S.; Lifshitz, C.; Rappoport, Z.; Karni, M.; Mandelbaum, A. *J. Am. Chem. Soc.* **1981**, *103*, 2869. (l) Biali, S.; Rappoport, Z. *Ibid.* **1984**, *106*, 477. (m) Biali, S.; Rappoport, Z. *Ibid.* **1984**, *106*, 5641. (n) Biali, S.; Depke, G.; Rappoport, Z.; Schwarz, H. *Ibid.* **1984**, *106*, 496. (o) Nugiel, D. A.; Rappoport, Z. *J. Am. Chem. Soc.* **1985**, *107*, 3669.

(2) (a) Holmes, J. L.; Terlouw, J. K.; Lossing, F. P. *J. Phys. Chem.* **1976**, *80*, 2860. (b) Holmes, J. L.; Lossing, F. P. *J. Am. Chem. Soc.* **1980**, *102*, 1591. (c) Holmes, J. L.; Lossing, F. P.; *Ibid.* **1980**, *102*, 3732. (d) Holmes, J. L.; Burgers, P. C.; Terlouw, J. K. *Can. J. Chem.* **1981**, *59*, 1805. (e) Holmes, J. L.; Lossing, F. P. *J. Am. Chem. Soc.* **1982**, *104*, 2648. (f) Back, R. A. *Can. J. Chem.* **1982**, *60*, 2537. (g) Terlouw, J. K.; Heerma, W.; Holmes, J. L.; Burgers, P. C. *Org. Mass Spectrom.* **1984**, *15*, 582.

(3) (a) Bouma, W. J.; MacLeod, J. K.; Radom, L. *Nouv. J. Chim.* **1978**, *2*, 439. (b) Bouma, W. J.; MacLeod, J. K.; Radom, L. *J. Am. Chem. Soc.* **1979**, *101*, 5540. (c) Bouma, W. J.; MacLeod, J. K.; Radom, L. *Ibid.* **1980**, *102*, 2246. (d) Frenking, G.; Heinrich, N.; Schmidt, J.; Schwarz, H. *Z. Naturforsch., B: Anorg. Chem., Org. Chem.* **1982**, *37*, 1597. (e) Bouchoux, G.; Hoppilliard, Y.; Jaudon, P. *Nouv. J. Chim.* **1982**, *6*, 43. (f) Bouchoux, G.; Flament, J. P.; Hoppiliard, Y. *Int. J. Mass Spectrom. Ion Processes* **1984**, *57*, 1597.

0002-7863/86/1508-0593$01.50/0